

# Research on Independent Driving Electric Vehicle in the Pivot Steering and Experimental Validation

Yue Zhao, Jun Ni and Jibin Hu,  
National Key Lab of Vehicular Transmission, Beijing  
Institute of Technology, ,  
BIT  
Beijing P. R. China,  
E-mail: [nijun\\_bit@bit.edu.cn](mailto:nijun_bit@bit.edu.cn)

**Abstract:** *In recent years, researchers concern the ability of the independent driving vehicle with the development of the electric vehicle. Hub-motor and wheel-side motor driving structure promotes the performance of vehicles. But most of the researchers only concern the improving in handing-stability and ignore the ability of pivot steering which highly improves the maneuverability. So in this paper, the pivot steering process of a rear driving vehicle equipped with wheel side motor has been researched. Based on a 7DOF math model and experiment of a prototype vehicle, dynamic feature of this process has been explored and the mechanism of the action has been found.*

**Key words:** *independent driving vehicle, pivot steering, wheel-side motor, Magic Formula, 7 DOF Model*

## I INTRODUCTION

With the development of the electric vehicle, drive structure has been largely improved. Equipped with wheel-side motor and hub motor, output torque can be easily controlled both in magnitude and vector direction. This gives more potential and flexibility to wheeled vehicles. Except the pivot steering function, the yaw moment control can be easily reached by controlling the motor output torque. And slip ratio control can be more precise. These technologies can improve the handing-stability and maneuverability of the vehicle.

This kind of layout is not rare but in the area of independent driving vehicle, researchers always concern the benefit it can bring for handing-stability. E. Esmailzadeh established a dynamic model for a 4WD motorized vehicle and analysis the simulation result [1]; J.-C. Fauroux's work is about improving the efficiency of skid steering through modify the distribution of the force on the wheel [2]; B. Maclaurin established a skid steering model with the Magic Formula [3] and compare the difference of skid steer and Ackermann steer and draw the conclusion that the skid-steered vehicle is generally neutral to over steer whereas the Ackermann-steered vehicle is understeer [4]; Y. Hori's research the influence of independent drive on

longitudinal and lateral dynamic through the UOT March II, the experimental vehicle build by his lab[5]; also, the direct yaw moment control method has been developed a lot for the torque generated by the independent driving motor can efficiently promote the performance of vehicle in many area [6]-[10].

But the promotion of maneuverability is seldom mentioned, which means the pivot steering process is ignored. Therefore, this article aims at analyzing the process of pivot steering of an independent driving vehicle.

Considering the cost and structure complexity, not all the independent driving vehicle is all-wheel-drive. For a rear-drive vehicle, the yaw moment is produced by the motor on rear axle. Hence the yaw moment will not locate in the geometry center. So, the turning center of the vehicle can't exist in the geometric center. To analysis the dynamic feature during the pivot steering, we build a 7 DOFs model to simulate the working condition, including the longitudinal, lateral and yaw DOF. To express the force of the tire accuracy, we use the "Magic Formula" as the tire model. With these above, we do the experiment of pivot steering in real to confirm the theory.

## II THE CONSTRUCTION OF DYNAMIC MODEL OF INDEPENDENT DRIVING VEHICLE

As we can imagine, the process of pivot steering is quite short and limited within a small space. Thus, the variation of the travel of suspension system can be very small. So we ignore the vertical displacement of each wheel and pitch and roll motion. Hence we assume the movement of the vehicle is limited on a flat surface.

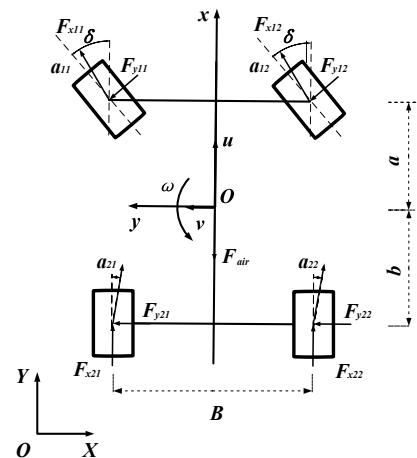


Fig. 1: 7 DOF Nonlinear Dynamic Model.

As mentioned above, the model is constructed by 7 DOFs, including the longitudinal, lateral and yaw motion of the body, as well as the rotation motion of four wheels.

All the physical parameters are defined in a local coordinate frame denoted by (o, x, y) assigned at the C.G. of the vehicle, showed in Fig. 1. The model of the vehicle's body is constructed according to the equilibrium along the longitudinal direction and lateral direction, as well as the torque balance around the Z axis, we give there equations below:

$$\begin{aligned} m(\dot{u} - v\omega) &= \sum_{i=1}^2 F_{xli} \cos \delta - \sum_{i=1}^2 F_{xli} \sin \delta + F_{x21} + F_{x22} \\ m(\dot{v} - u\omega) &= \sum_{i=1}^2 F_{xli} \sin \delta - \sum_{i=1}^2 F_{xli} \cos \delta + F_{y21} + F_{y22} \\ I_z \dot{\omega} &= \left[ \sum_{i=1}^2 F_{xli} a \sin \delta + \sum_{i=1}^2 F_{yli} a \cos \delta + \sum_{i=1}^2 F_{yli} \frac{B}{2} \sin \delta \right] \\ &\quad + (F_{x21} - F_{x22}) \frac{B}{2} - (F_{y11} + F_{y12}) b \end{aligned} \quad (1)$$

Where:  $m$  is the mass of the vehicle;  $u$  is the longitudinal velocity of the vehicle;  $v$  is the lateral velocity of the vehicle;  $\omega$  is the yaw velocity of the vehicle;  $\delta$  is the front wheel steering angle;  $I_z$  is the yaw inertial of the vehicle;  $a, b$  are the distance from C.G location to front and rear axle respectively;  $B$  is wheel track;  $F_{xii}, F_{yii}$  are the longitudinal and lateral force of individual tires as Fig. 1 shown.

The model of wheel consist two parts, including rotating movement of the wheel and the force of the tire. The rotating movement is expressed by the equation below:

$$J\dot{\omega}_i = T_{di} - T_{bi} - F_{xi} R_w - F_{zi} R_w f \quad (2)$$

Where:  $J$  is the yaw inertial of the wheel;  $\omega_i$  is the yaw velocity of each wheel;  $T_{di}$  is the driving torque of the wheel;  $T_{bi}$  is the break torque of the wheel;  $F_{xi}, F_{zi}$  are the longitudinal force and vertical load of each wheel respectively;  $R_w$  is the radius of each wheel, which is assumed to be equal;  $f$  is the rolling friction coefficient.

And the force on tire is described by "the Magic Formula".:

$$F = D \sin \{ C \arctan [ BX - E ( BX - \arctan ( BX ) ) ] \} \quad (3)$$

This equation could both represent the lateral and longitudinal working condition. So the parameters in the equation might have different meaning in different condition respectively. Where:  $F$  is the lateral force or longitudinal force;  $X$  is lateral side slip angle or longitudinal slip ratio; while  $B, C, D, E$  are constant parameters, which are obtained by fitting the test data. Hence, the input of the tire model consists of two parts: the  $X$ , which is lateral side slip angle or longitudinal ratio and vertical load of the tire.

The tire used in this vehicle is Hoosier 18×6-10 compound R25B. The tire test data of Hoosier 18×6-10 R25B was obtained with support of FSAE Tire Test Consortium (TTC).

Based on enough testing data, we could get the model of the non-linear part of the tire force, shown in Fig. 2 below.

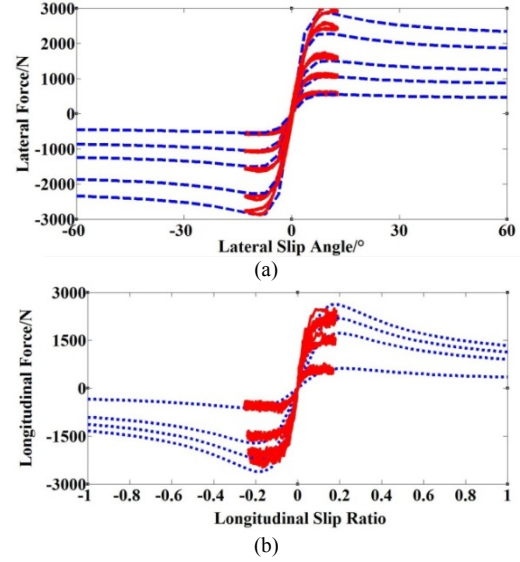


Fig. 2: The chart of the tire test data. Graph (a) shows the lateral data and graph (b) shows the longitudinal data.

We should notice that, however, the result showed in Fig. 2 is only the pure-condition model, which happens quite rare in the real case. So we need to build a combined-condition model that can be expressed as the equation below:

$$\begin{cases} F_x = \frac{s}{\sqrt{s^2 + \tan^2 \alpha}} F_{x0} \\ F_y = \frac{s}{\sqrt{s^2 + \tan^2 \alpha}} F_{y0} \end{cases} \quad (4)$$

Where:  $F_x$  and  $F_y$  are the combined-conditioned longitudinal and lateral tire force;  $F_{x0}$  and  $F_{y0}$  are the pure-conditioned longitudinal and lateral force;  $s$  is the slip ratio of the wheel;  $\alpha$  is the side slip angle of the tire.

As we said above, side slip angle and longitudinal slip ratio are one part of the input of the tire model. These two parameters are defined as below:

$$\alpha_{11} = \delta - \arctan \left( \frac{v + a\omega}{u - \frac{B}{2}\omega} \right) \quad (5)$$

$$\alpha_{12} = \delta - \arctan \left( \frac{v + a\omega}{u + \frac{B}{2}\omega} \right) \quad (6)$$

$$\alpha_{21} = \arctan \left( \frac{b\omega - v}{u - \frac{B}{2}\omega} \right) \quad (7)$$

$$\alpha_{22} = \arctan \left( \frac{b\omega - v}{u + \frac{B}{2}\omega} \right) \quad (8)$$

Where:  $\alpha_{ij}$  is the side slip angle of the tire,  $i$  is the axle number of the vehicle,  $j$  represents the left and right; other parameters are the same as above equation.

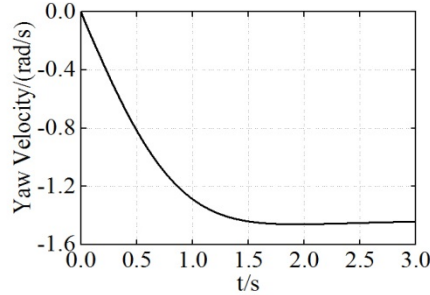
$$s = \begin{cases} \frac{v_{xi} - \omega_{ei}}{v_{xi}} > 0 & \text{break condition} \\ \frac{v_{xi} - \omega_{ei}}{\omega_{ei}} < 0 & \text{drive condition} \end{cases} \quad (9)$$

Where:  $s$  is the slip ratio, rest of the parameters are the

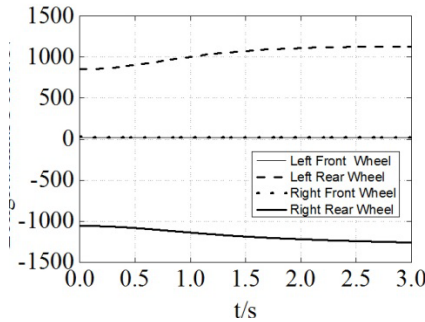
same as above.

### III ANALYSIS OF THE SIMULATION RESULT OF PIVOT STEER

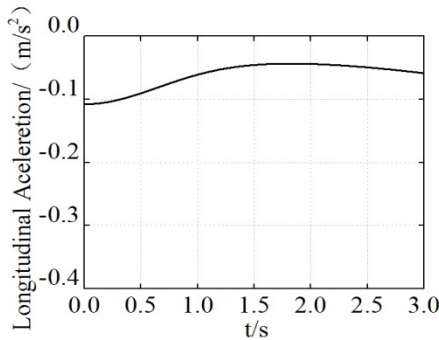
The math model mentioned above is constructed in MATLAB. The results of the simulation are shown below:



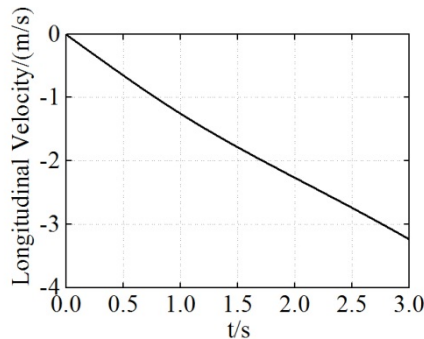
(a) Yaw Velocity



(b) Longitudinal Force



(c) Longitudinal Acceleration



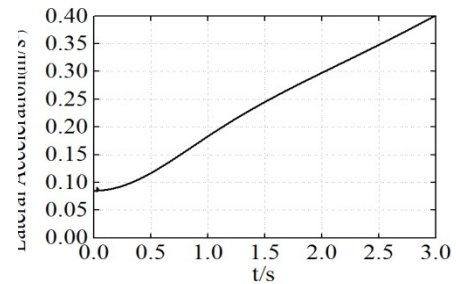
(d) Longitudinal Velocity

It is obvious the front wheel without steering will cause a great drag force. Therefore, the drive torque must be big enough to overcome this resistance torque. Through the simulation process we could find that 300 N.m can offer enough drive force. The results are shown in Fig. 3.

Fig. 3(a), is the variation of yaw velocity through the steer process. During the steer process, the yaw velocity rise first and become steady but has a little decline. This variation will influence the track of the vehicle. Mainly cause a difference on the curvature of the track.

As we can infer, the yaw velocity is caused by the yaw moment generated by the opposite input torque. These torque give the opposite direction forces and we can observe the force in Fig. 3(b). We should notice that the longitudinal force of rear wheels, which is the drive force, is different between left and right wheel in value. This difference will make the resultant force in the longitudinal direction nonzero and make the vehicle move in this direction. Therefore, under the effect of a velocity in the longitudinal direction and a yaw velocity, the vehicle will rotate around a certain point outside the body, which is the center of the rotation.

Besides the effect on motion type, the difference of left and right rear wheel also affects the longitudinal speed and acceleration. As the resultant force is nonzero, the vehicle will accelerate in the longitudinal direction through the steer process. We could observe this tendency in Fig. 3(c) and Fig.3(d). However, the value of longitudinal acceleration is variable and exist a peak in the graph. This variation is related to the variation of the difference between the left and right rear wheels. The variation of the resultant force can be seen in Fig. 3(f).



(e) Lateral Acceleration

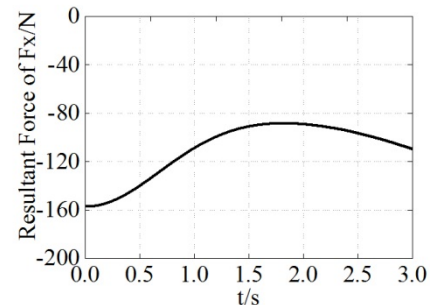
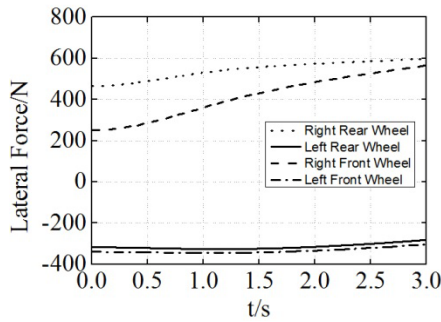
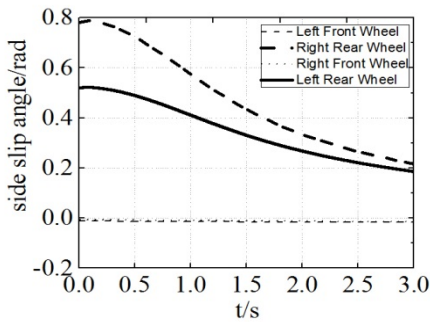


Fig. 3: Results of the Simulation with 300N.m Input Torque

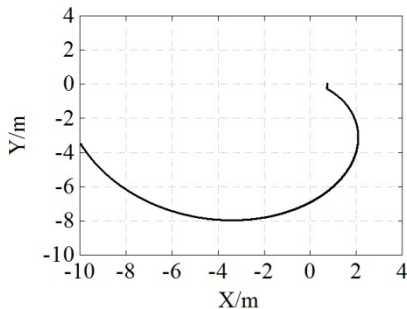
(b) Resultant Force in Longitudinal Direction



(c) Lateral Force



(d) Side Slip Angle



(e) Track of C.G

Fig. 4: Results of the Simulation with 300N.m Input Torque

And from the analysis above we could know, the motion of the vehicle is a circling motion rather than a standard pivot steer. So with the raise of the longitudinal speed, the lateral acceleration will also rise up and we could observe in Fig. 4 (a). Also, the lateral acceleration will cause the load transfer and this is the reason for the difference of rear wheel's longitudinal force. As the load on the wheel differs from each other, the drive force will differ from each other. Also we should notice the load transfer will always make the vehicle has a backward speed because the location of the center of rotation is determined by the direction of the yaw velocity. In Fig. 5 we could see, the center of rotation is always on the opposite side of backward drive force. This will make the load transfer to the backward force side and make this side a bigger drive force. That's the reason why the vehicle will always go backward.

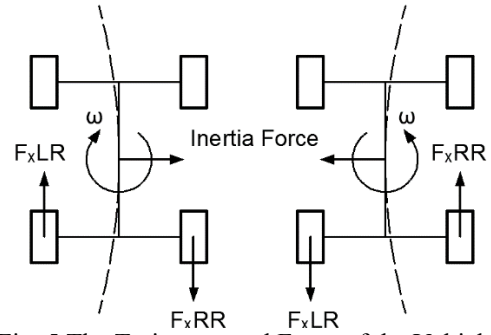


Fig. 5 The Trajectory and Force of the Vehicle

In Fig. 4(d), the curve of side slip angle of rear wheel has an obvious variation in value. As we know, the side slip angle is defined by the quotient of longitudinal and lateral velocity on the wheel. So it can be affected by the track of the vehicle. And in Fig. 4(e), we could observe the track of the vehicle's C.G. The track of the vehicle's curvature is getting smaller. Under this kind of tendency, the lateral speed of the vehicle is getting smaller than the longitudinal speed. Therefore, the side slip angle will decrease with the vehicle's steering.

#### IV THE EXPERIMENT OF PIVOT STEER

As we get the tire test data, we could have a more accurate simulation data. So we could make the results of the simulation and experiment proves each other. That is the reason why we need to carry out the experiment.

The vehicle used for experiment is a prototype vehicle equipped with a GPS/INS system, which can collect the location and gesture information of the vehicle.

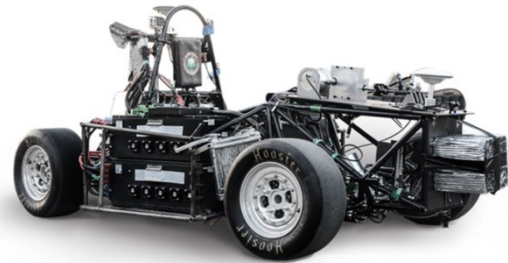


Fig. 6 The prototype vehicle used in the experiment. The front bridge still conserve the Ackermann steering structure, but the rear bridge is constructed by two electric motors and corresponding reducer, which can drive the rear wheel independently.

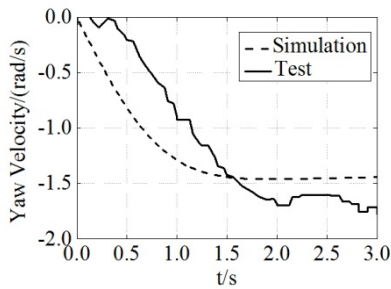
The wheel side electric motor we used is ERMAX 207. The peak power of this motor is 70kw and the peak output torque is 160Nm. To make the speed and acceleration performances fulfill demand of a race car, the prototype vehicle equipped with an epicycle gear reducer, which has a ratio of 4.



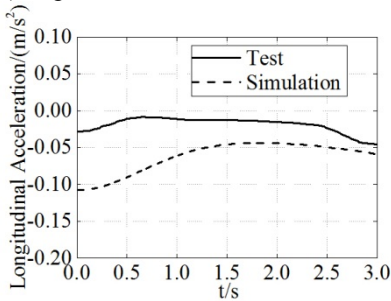


Fig. 7 The motor and inverter used on the prototype vehicle

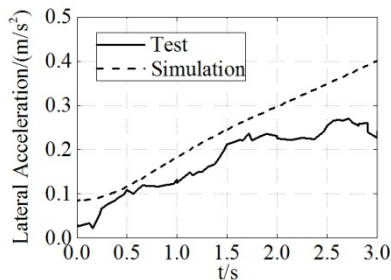
The advantage of this type of layout is that driver can choose the steering type depending on the situation: when driving in normal cornering state, the vehicle can remain the Ackermann steering model, still the motor can give a direct yaw moment to the vehicle to control the vehicle and improve the handing stability; when the driving space doesn't allow the vehicle turning in Ackermann way, the vehicle can do pivot steer through giving opposite driving force by the motor individually. We can see this kind of layout could combine the advantage of skid steering and Ackermann steering in dynamic.



(a) Experiment Result of Yaw Velocity



(b) Experiment Result of Longitudinal Acceleration



(c) Experiment Result of Lateral Acceleration

Fig. 8: The Result of Experiment. The experiment is carried by the prototype vehicle, which has different drive torque

on the drive wheel and the front wheel remain still during the experiment process.

From Fig. 8 (a), we can see the yaw velocity basically keep the same trend with the simulation results. The yaw velocity goes down first and then keeps steady at some certain value. Also, in Fig. 8 (b) and Fig. 8 (c), we can observe the other parameters, such as longitudinal acceleration and lateral acceleration, have the same trend as the simulation results. However, the values of the simulation results and experiment results have a little difference. We could see the yaw velocity in experiment is bigger than the simulation results. However, except the yaw velocity, all the other parameters from the experiment are smaller than the simulation results.

In the experiment, the smallest drive torque that can drive the vehicle in the experiment is smaller than the simulation data. This is mainly caused by the tire. The tire used in this vehicle is Hoosier 18×6-10 compound R25B. This is a racecar tire which needs a suitable temperature to keep at a high adhesion condition. So the adhesion coefficient varies with the temperature obviously. From this we could conduct that the adhesion condition of the experiment is much different compared to the adhesion condition of the tire test. Because the slip ratio of rear wheels remains at -1 during the pivot steering process according to the analysis above, which means the value of longitudinal force will remain at a very small value whether the adhesion condition changes or not. Since the traction force varies in a small range, we deem the reason caused yaw velocity increase is decreasing of resistance force, which is the lateral force on the wheel. For this reason, the vehicle is much easier to have a motion on the ground with a same or smaller drive torque.

These differences finally reflect on the data of acceleration and yaw velocity. The yaw velocity will stable at a higher value at the end of pivot steering process because of the decreasing lateral force causing a rise of angular acceleration. Besides the effect on yaw velocity, the decreasing of resistance also affects lateral and longitudinal acceleration. Due to the drive wheel is at back axle, the rotate center doesn't locate at the gravity center of the vehicle. Therefore, the side slip angle of front axle is different from that of back axle, which equals the difference of lateral force. This distinction forms the resultant force on lateral direction. As the decrease of lateral force is caused by the change of adhesion coefficient, the decrease between back and front axle won't differ a lot, which means the resultant force will also decline. This decline equals the decline of lateral acceleration. Since the lateral acceleration is different, the load transfer will be influenced by the lateral acceleration. And the longitudinal acceleration descends with the load transfer.

## V CONCLUSION

In this paper, a dynamic model of pivot steering implemented on an independent driving vehicle is established and matching experiment is carried out. From the results of simulation and experiment, we could find that for a two wheel drive independent driving vehicle, it can't just turn on a spot as imagine. Furthermore, even the drive torque of the drive wheel is the same, the vehicle still will move on a specific direction rather than stay at a certain point.

## REFERENCE:

- [1] E. Esmailzadeh, G.R. Vossoughi, A. Goodarzi, "Dynamic Modeling and Analysis of a Four Motorized Wheels Electric Vehicle", *Vehicle System Dynamics* 2001, Vol. 35, No. 3, pp. 163-194
- [2] J.-C. Fauroux, P. Vaslin "Modeling, experimenting and improving skid steering on a 6×6 all-terrain mobile platform", *J. Field Rob.*, vol. 27, pp. 107-126, 2010.
- [3] B. Maclaurin, "A skid steering model using the Magic Formula", *Journal of Terramechanics* 48 (2011) 247–263
- [4] B.Maclaurin, "Comparing the steering performances of skid and Ackermann steered vehicles", *Proc. Inst. Mech. Eng., PartD: J. Automobile Eng.*, vol.222, pp.739-756, 2008.
- [5] Y. Hori "Future vehicle driven by electricity and control-research on four-wheel-motored UOT Electric March II"" *IEEE TRANSACTIONS ON INDUSTRIAL ELECTRONICS*, VOL. 51, NO. 5, OCTOBER 2004
- [6] V. Ivanov, D. Savitski, J. Orus, J. M. R. Fortun, "All-Wheel-Drive electric vehicle with on-board motors: experimental validation of the motion control systems", *IECON2015-Yokohama* November 9-12, 2015.
- [7] C. Feng, N. Ding, Y. He, "An integrated control algorithm of ABS and DYC for emergency braking on a  $\mu$ -Split road", 2012 International Conference on Control Engineering and Communication Technology.
- [8] "Crusher unmanned ground combat vehicle unveiled", *Defense Advanced Research Projects Agency*. 2010.
- [9] S. Gao, N. Cheung and K.W.Eric. "Skid steering in 4-wheel-drive electric vehicle", *IEEE Int. Con. Power Electronics and Drive Sys*, 2007.
- [10] W. R. Meldrum, F. B. Hoogterp, A. R. Kovnat, "Modeling and simulation of a differential torque steered wheeled vehicle", *U.S Army Research Report*, 2002.